Innovative Prediction of Vehicle Position Based on Closed Loop Modeling of Capacitive Accelerometer

Conference Paper · May 2019

DOI: 10.1109/ICSIoT47925.2019.00017

3 authors:

Mamudu Hamidu
Kumasi Technical University, Kumasi Ghana
8 PUBLICATIONS **6** CITATIONS
SEE PROFILE

Kponyo Jerry
Kwame Nkrumah University Of Science and Technology
56 PUBLICATIONS **334** CITATIONS
SEE PROFILE

Amevi Acakpovi
Accra Technical University
99 PUBLICATIONS **415** CITATIONS
SEE PROFILE

Innovative Prediction of Vehicle Position Based on Closed Loop Modeling of Capacitive Accelerometer

Mamudu Hamidu
Department of Electrical/Electronic Engineering
Kumasi Technical University
Kumasi, Ghana
Email: drsennet@gmail.com

Jerry John Kponyo
Department of Electrical/Electronic Engineering
Kwame Nkrumah University of Science and Technology
Kumasi, Ghana
Email: jjkponyosoe@knust.edu.gh

Amevi Acakpovi
Department of Electrical/Electronic Engineering
Accra Technical University
Accra, Ghana
Email: acakpovia@gmail.com

Abstract- This paper presents a novel model of a closed loop capacitive accelerometer. Capacitive accelerometer is able to detect the displacement/position of a vehicle by means of Position-Velocity-Acceleration (PVA) model. The closed loop design is design to overcome the steady state error obtained in the equivalent open loop design. Therefore, in this paper, a parallel Proportional Integral Derivative (PID) controller with a derivative filter is designed to establish a unity feedback accelerometer for the purpose of reducing or eliminating the steady state error. The accelerometer gave an exact linear dependence of displacement on a step-like function of acceleration signal input. Matlab/Simulink software was used to design the control system and construct the overall proposed mathematical model. Test show that, for acceleration value of ±1 gravity (g) produces displacement of ±1 meter (m). The system produces an initial spike with a transient time of less than 0.1 secs. This is same for an acceleration of ±10 g. The use of PID controller with a derivative filter in this paper provide a significant improvement in predicting the linear dependence relationship between acceleration and displacement than the traditional approach of continuous tuning of PID for accelerometer system stability.

Keywords-Accelerometer; position-velocity-acceleration; PID-controller; modelling; closed loop.

I. INTRODUCTION

The use of accelerometer sensor in the field of vehicle tracking is predominantly for the determination of a vehicle's acceleration. The obtained acceleration can therefore be mathematically computed into knowing the velocity and the position of the vehicle. However, to be able to detect the acceleration of a vehicle, there is a readout mechanism to integrate. The readout out mechanism can be in the form of capacitive [8], [9], [10], [11], [12], [13], [14], piezoelectric [15], [16], [17], piezo-resistive [1], and thermal [18], [19].

The choice of capacitive accelerometer in vehicle tracking is normally based on its advantages such as: static biasing been zero, high sensitivity ability, and better thermal stability. These advantages make capacitive accelerometer, the best choice for lower-power applications [20].

The use of accelerometer in aiding measurements of vehicles' position via Global Position System (GPS) is achieved with the use of three-axis capacitive designed IC. This design has uniform sensitivity to three axes developed through the micromachinery technique [2], [3]. The structure of this sensor is characterized by a glass-silicon-glass produced from a mass-bonded to a surrounding silicon support which is suspended only at the center pillar with four thin silicon beams. The suspending silicon mass proof measures parallel movement in z-acceleration and when tilted, it measures the X or Y axis acceleration through means of capacitance. The measurement of capacitance is by means of connection of silicon electrodes on the plate of the mass proof in order to make movements through four capacitors whenever there is a parallel shift or tilt. By this technique, the three-axis components of acceleration are generated in X, Y, and Z axis (a_x, a_y, a_z) by measuring capacitances [6].

Based on this primary micro-machining, readout circuits are developed to record the acceleration of a vehicle while noting that, two important parameters are required to determine the vehicle state (velocity and position). Therefore, Position-Velocity-Acceleration (PVA) model is explored for the conversion from acceleration into velocity and position respectively. The velocity is obtained through the first integration of the acceleration whilst the position (distance) is obtained through the second integration. For accuracy purposes, measured acceleration should correspond to the distance travelled by the vehicle. This is evident as a linear dependence relationship between acceleration and distance of the vehicle [4], [5].

However, in open loop analysis and simulations, using self-tuning step function, acceleration input shows a high error margin in achieving the position even though its relationship is still linear dependent. This means that, a controller is needed to check the accuracy of the system measurements for velocity and position. Therefore, in other to fuse GPS and accelerometer to achieve effective vehicle location, a closed loop mechanism is adopted in this paper and mathematically modelled simulated using Matlab/Simulink software.

II. OPEN LOOP ACCELEROMETER SYSTEM

The linear time variant (LTV) model of open loop accelerometer without change in capacitance is represented in (1) [21], [22], [223], [25]:

978-1-7281-7417-4/19/$31.00 ©2019 IEEE
DOI 10.1109/ICSIoT47925.2019.00017

$$
\left.\begin{aligned}
m\,\frac{d^2x}{dt^2} &= kx + b\,\frac{dx}{dt} + m\,\frac{dx^2}{dt^2}\\
b &= \tfrac{1}{2}\mu A^2\left[\frac{1}{(d_0-d_x)^3}+\frac{1}{(d_0+d_x)^3}\right]\\
\frac{d^2y}{dt^2} &= \frac{d^2y}{dt^2} - \left[\frac{k}{m}x + \tfrac{1}{2}\mu A^2\left[\frac{1}{(d_0-x)^3}+\frac{1}{(d_0+x)^3}\right].\frac{dx}{dt}\right] + \frac{\varepsilon_0 A V_1^2}{4m}.x\\
a &= \frac{d^2y}{dt^2}\\
a &= \frac{d^2x}{dt^2} + \left[\frac{\mu A^2}{{d_0}^3}.\frac{dx}{dt}\right] + x.\left[\frac{k}{m} - \frac{\varepsilon_0 A V_1^2}{4m}\right]
\end{aligned}\right\} \quad (1)
$$

Where:

b : damping coefficient is due to the spring or viscous displacement

μ: Air gap displacement as a result of vehicle

A : Mobile plaque area

$(d_0,\ d_x)$: Distance between fixed electrodes

Applying the Laplace transfer function (2) is obtained:

$$
\left.\begin{aligned}
s^2.X(s) + \left[\frac{\mu A^2}{{d_0}^3}.s\right].X(s) + X(s).\left[k - \frac{\varepsilon_0 A V_1^2}{d_0^2}\right] &= a(s).m\\
G_{ME}(s) = \frac{X(s)}{a(s)} &= \frac{1}{\left(s^2 + \left[\frac{\mu A^2}{m.{d_0}^3}.s\right] + \left[\frac{k}{m} - \frac{\varepsilon_0 A V_1^2}{m.d_0^2}\right]\right)}
\end{aligned}\right\} \quad (2)
$$

$G_{ME}(s)$: Feed forward Gain of Mechanical and Electrostatic Model

The open loop block diagram with electronic readout circuit (Accelerometer gain detection and demodulation with low pass filter (LPF)) [4], [21], [22], [23], [24], is in figure 1.

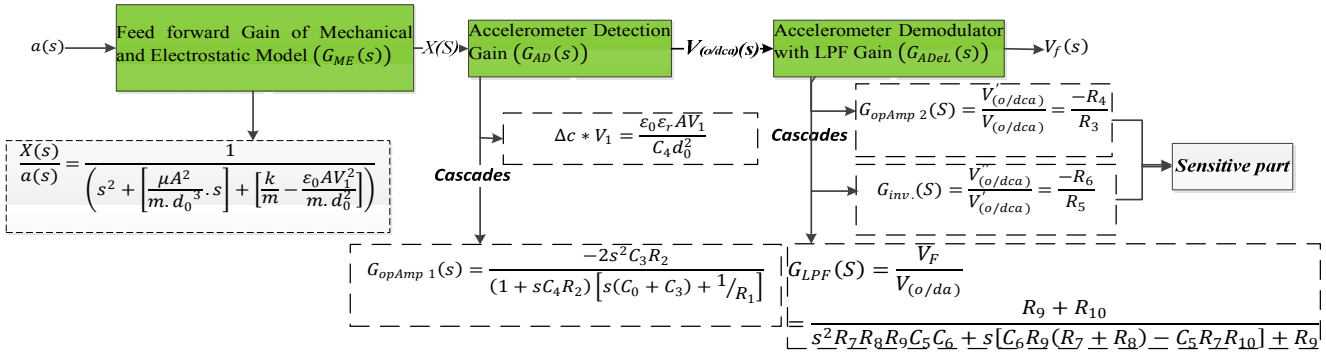

Figure 1: open loop accelerometer system with readout components

(G_{AD}) : Accelerometer Detection Gain

$G_{opAmp1}(s)$: Accelerometer Detection Operational Amplifier Gain

$G_{ADeL}(s)$: Accelerometer Demodulator with LPF Gain

$G_{opAmp2}(S)$: Electronic Read-out Operational Amplifier Gain

$G_{inv.}(S)$: Electronic Read-out inverter Gain

$G_{LPF}(S)$: Electronic Read-out Low Pass Filter Gain

$V_F(s)$: Approximate displacement of x

Accelerometer detection block has a gain of (G_{AD}) which is obtained from the measurement of capacitance principle of electrostatic force. Its purpose is to transform the mechanical displacement into electronic measurements due to changes in capacitance. The acceleration detection unit has a capacitor with voltage applied to both sides of its plate. Displacement measurements are obtained through a suspension of a metallic rod between the capacitor with difference in rod distances taking into consideration.

The signal, $V_{(o/dca)}$obtained at the output of the detection unit is filtered using LPF in the Accelerometer Demodulator unit of the block diagram in figure 1.

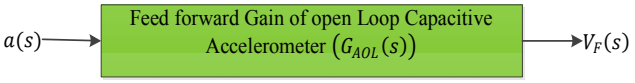

Figure 2: Feed forward Gain of open Loop Capacitive Accelerometer $(G_{AOL}(s))$

In figure 2, a generalized model of $(G_{AOL}(s))$ is represented in (3) as a cascade of $(G_{ME}(s)), (G_{AD}(s))$ and $(G_{ADeL}(s))$.

$$G_{AOL}(s) = (G_{ME}(s)) * (G_{AD}(s)) * (G_{ADeL}(s)) \quad (3)$$

From figure 2, the open loop transfer function is represented in (4):

$$\Rightarrow G_{AOL}(s) = \frac{V_F(s)}{a(s)} \ \&\ V_f(s) = G_{AOL}(s)a(s) \quad (4)$$

Equation 5 represents the overall model of the open loop accelerometer factoring in the mechanical model, displacement detection and the readout circuit (demodulator) model in Figure 1.

$$
\left.
\begin{aligned}
V_F(s) \equiv V_{\left(\frac{o}{dca}\right)}(s) * G_{ADeL}(s) &= \left(V_{\left(\frac{o}{dca}\right)}(s)\right) * \left(G_{inv.}(s) * G_{opAmp2}(s)\right) * (R_9 + R_{10}) \\
V_{(o/dca)} &= \frac{1}{T}\left[\int_0^{\frac{T}{2}}\left(V_1(t)\right)dt - \int_{\frac{T}{2}}^{T}\left(V_1(t)\right)dt\right] * [\Delta C * x] \\
V_1(t) &= V_1 \sin(\omega t) \\
V_{(o/dca)} &= \frac{1}{T}\left[\int_0^{\frac{T}{2}}\left(V_1\sin(\omega t)\right)dt - \int_{\frac{T}{2}}^{T}\left(V_1\sin(\omega t)\right)dt\right] * [\Delta C * x] \\
\therefore V_{(o/dca)} &= \frac{1}{T}\left[\int_0^{\frac{T}{2}}\left(V_1\sin(\omega t)\right)dt - \int_{\frac{T}{2}}^{T}\left(V_1\sin(\omega t)\right)dt\right] * \left[\frac{\varepsilon_0 \varepsilon_r A}{C_4 d_0^2} * x\right] \\
\text{solving, } V_{(o/dca)} &\gg \frac{4V_1}{T\omega}\left[\frac{\varepsilon_0 \varepsilon_r A}{C_4 d_0^2} * x\right] \\
\therefore V_f(s) &= \frac{4V_1}{T\omega}\left[\frac{\varepsilon_0 \varepsilon_r A}{C_4 d_0^2} * x\right] * \left[\left(G_{inv.}(s) * G_{opAmp2}(s)\right) * (R_9 + R_{10})\right] \\
\text{Finally; } V_F(s) &= \frac{4V_1}{\pi}\left[\frac{\varepsilon_0 \varepsilon_r A}{C_4 d_0^2} * x\right] * \left[\left(G_{inv.}(s) * G_{opAmp2}(s)\right) * (R_9 + R_{10})\right]
\end{aligned}
\right\} (5)
$$

The final open loop model of the capacitive accelerometer $V_f(s)$ is put into a functional block diagram in figure 3.

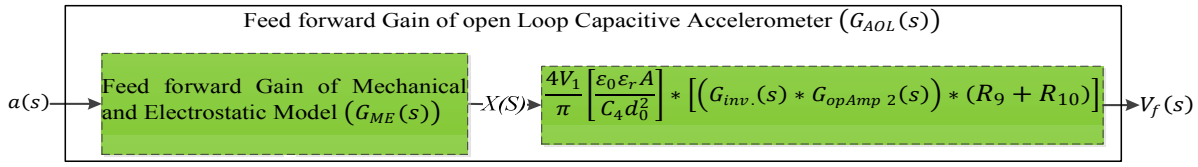

Figure 3: functional block of accelerometer open loop structure of (5)

Finally, the open loop transfer function is represented in this paper in (6):

$$
\left.
\begin{aligned}
G_{AOL}(s) &= \frac{G_{ocf}1}{\left(s^2 + \left[\frac{\mu A^2}{m.{d_0}^3}.s\right] + \left[\frac{k}{m} - \frac{\varepsilon_0 A V_1^2}{m.d_0^2}\right]\right)} \\
G_{AOL}(s) &= \frac{7.436e10}{s^2 + 316.1\,s + 1.016e0\,4}
\end{aligned}
\right\} (6)
$$

The next section analyses how the closed loop capacitive accelerometer is designed with the use of Proportional-Integral-Differential (PID) controller.

III. Closed Loop Accelerometer Modeling

A closed loop system is generally a method of automatic system control in which operation, process, or mechanism is self-regulating by mean of feedback. In this section, the analytical development of feedback signal is considered and use of PID controller is analyzed.

A. Development of the feedback loop for capacitive accelerometer

The need for a feedback loop is to help remove the oscillatory nature of the $V_f(s)$. This makes the measurements from the accelerometer highly unstable. Therefore, there is the need to control the output signal. Using the accelerometer in a vehicle depends on high frequency of about $100 \times 10^3 H_z$ which have to be controlled for proper estimation of $V_f(s)$. Based on this anomaly, this research looks at the Proportional Integral Derivative (PID) controller. The PID would help the accelerometer to achieve better response stability over time to aid the vehicle tracking system with position accuracy before interfacing it with a Kalman filter.

B. Choosing Feedback signal

According to [7], in order to obtain a feedback system, one has to select a sensor, and this sensor should provide an output voltage proportional to the dynamic model. Therefore, in choosing the feedback signal, a balancing force is needed to check the inertial force of the accelerometer. This balancing force is called the electrostatic force. It is chosen because it establishes the reading of small displacement from the proof mass between the two fixed electrodes on the parallel plates. Therefore, any feedforward force, the feedback will be the electrostatic forces acting on both the positive and negative polarities. Also, the electrostatic forces are used to provide a restoration of force to balance acceleration force. Figure 4 shows the representation of the accelerometer closed loop structure.

[1] G_{ocf}: open loop cascade factor $= \left[\frac{4V_1}{\pi}\left(\frac{\varepsilon_0 \varepsilon_r A}{C_4 d_0^2}\right)\right] * \left[\left(G_{inv.}(s) * G_{opAmp2}(s)\right) * (R_9 + R_{10})\right]$

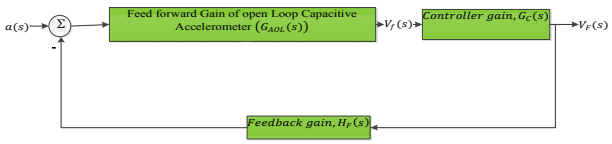

Figure 4: closed loop structure of accelerometer

To establish the feedback force, a bias supply signal is introduce V_b with excitation signal v_1 to obtain a feedback signal V_F to the two electrodes. This generates the V_{ne} and V_{pe} as negative electrode and positive electrode supplies respectively. This is represented in (7) as:

$$\left.\begin{aligned} V_{ne} &= v_1 - V_b + V_F \\ V_{pe} &= v_2 + V_b + V_F \end{aligned}\right\} \& \left.\begin{aligned} v_1 &= V_1 \sin\omega t \\ v_2 &= -V_1 \sin\omega t \end{aligned}\right\} \quad (7)$$

The resultant signal gives (8):

$$V_{npe} = V_{ne} - V_{pe} \quad (8)$$

The application of the electrostatic force feedback gives (9):

$$\left.\begin{aligned} F_{el_F} &= F_{el_{ne}} + F_{el_{pe}} \\ F_{el_F} &= \frac{\varepsilon_0 \varepsilon_r A}{4} \cdot \left[\frac{V_{ne}^2}{(d_0 - d_x)^2} - \frac{V_{pe}^2}{(d_0 + d_x)^2}\right] \\ F_{el_F} &= \frac{\varepsilon_0 \varepsilon_r A}{4} \cdot \left[\frac{(V_1 sin\omega t - V_b + V_F)^2}{(d_0 - d_x)^2} - \frac{(-V_1 sin\omega t + V_b + V_F)^2}{(d_0 + d_x)^2}\right] \end{aligned}\right\} \quad (9)$$

The accelerometer having high system frequency and considering the initial position of the proof mass, the electrostatic force feedback mean signal is represented mathematically in (10):

$$F_{el_F} = \frac{1}{T}\int F_{el_F} dt = \frac{2\varepsilon_0 \varepsilon_r A}{{d_0}^3} \cdot \int [x(V_1 \sin\omega t - V_b + V_F)^2 - (-V_1 \sin\omega t + V_b + V_F)^2]\, dt \quad (10)$$

Expanding and integrating all terms with respect to t gives:

$$\left.\begin{aligned} F_{el_F} &= \frac{2\varepsilon_0 \varepsilon_r A}{{d_0}^3}\left[x\left(\frac{V_1^2}{2} + V_b^2 + V_F^2\right) - V_b V_F d_0\right]; \\ &\text{with inertial displacement of } x = 0 \\ \therefore \text{ the feedback electrostatic force, } F_{el_F} &= -\frac{2\varepsilon_0 \varepsilon_r A V_b V_F}{{d_0}^2} \end{aligned}\right\} \quad (11)$$

Rewriting the equations again for all the acting forces on the proof mass the feedback sensor gives (12):

$$\left.\begin{aligned} \vec{F}_i &= \vec{F}_e + \vec{F}_a + \vec{a}_x - F_{el_F} \\ ma = kx + \frac{1}{2}\mu A^2 &\left[\frac{1}{{d_0}^3} + \frac{1}{{d_0}^3}\right]\frac{dx}{dt} + m\frac{d^2x}{dt^2} + \frac{2\varepsilon_0 \varepsilon_r A V_b V_F}{{d_0}^2} \\ ma = kx + &\left[\frac{\mu A^2}{{d_0}^3}\right]\frac{dx}{dt} + m\frac{d^2x}{dt^2} + \frac{2\varepsilon_0 \varepsilon_r A V_b V_F}{{d_0}^2} \\ a = \frac{k}{m}x + \frac{1}{m}&\left[\frac{\mu A^2}{{d_0}^3}\right]\frac{dx}{dt} + \frac{d^2x}{dt^2} + \frac{1}{m}.\frac{2\varepsilon_0 \varepsilon_r A V_b V_F}{{d_0}^2} \end{aligned}\right\} \quad (12)$$

The model for feedforward including the controller in figure 5 becomes (13):

$$V_F(s) = V_f(s) * G_C(s) \Rightarrow V_F(s) = \left(G_{AOL}(s)\right) * \left(G_C(s)\right) \quad (13)$$

∴the close Accelerometer Loop Transfer function (G_ACL (s)) is:

$$\left.\begin{aligned} G_{ACL}(s) &= \frac{V_F(s)}{a(s)} = \frac{(G_{AOL}(s)) * (G_C(s))}{1 + (G_{AOL}(s)) * (G_C(s)) * (H_F(s))} \\ G_{ACL}(s) &= \frac{\left[\frac{7.436e10}{s^2 + 316.1\,s + 1.016e0\,4}\right] 2 * (G_C(s))}{1 + \left[\frac{7.436e10}{s^2 + 316.1\,s + 1.016e0\,4}\right] * (H_F(s))} \\ G_{ACL}(s) &= \frac{(7.436e10) * (G_C(s))}{[s^2 + 316.1\,s + 1.016e0\,4] + (7.436e10) * (G_C(s)) * (H_F(s))} \end{aligned}\right\} \quad (14)$$

C. Tuning of PID controller

i. Tuning

Controller term $G_C(s)$, which is the Proportional-Integral-Derivative (PID) is to control accelerometer output to the desirable value. This controller can be represented in PI, PD and PID action to fine-tune signals to desirable limits. The parallel model is used in controlling the accelerometer model in this paper. The controller transfer function is:

$$\left.\begin{aligned} G_c(s) &= K_p + \frac{K_i}{s} + K_d s \\ G_c(s) &= \frac{K_d s^2 + K_p s + K_i}{s} \end{aligned}\right\} \quad (15)$$

The PID controller transfer function in equation 15 is substituted in the accelerometer closed loop transfer function in (14) to obtain equation (16).

Expanding and grouping like terms of the root characteristics of the closed loop accelerometer (16) function gives (17).

$$\left.\begin{aligned} G_{ACL}(s) &= \frac{(G_{ocf}) * \left(\frac{K_d s^2 + K_p s + K_i}{s}\right)}{[s^2 + 316.1\,s + 1.016e0\,4] + (G_{ocf}) * \left(\frac{K_d s^2 + K_p s + K_i}{s}\right) * (H_F(s))} \\ G_{ACL}(s) &= \frac{(G_{ocf}) * (K_d s^2 + K_p s + K_i)}{[[s^2 + 316.1\,s + 1.016e0\,4]]s + (G_{ocf}) * (K_d s^2 + K_p s + K_i) * (H_F(s))} \end{aligned}\right\} \quad (16)$$

The root characteristics are of the third order and hence three poles will be obtained. Therefore, the three poles would be assumed to be stable by lying in the left-hand side of the s-plane. In other to establish better relationship with stability of the root characteristics all, the poles are assumed to be critically damped and should be $-1, -1, -1$.

$$\left.\begin{aligned} &[1.016e0\,4s + 316.1s^2 + s^3] + [(G_{ocf}) * (K_d s^2 + K_p s + K_i) * (H_F(s))] = 0 \\ s^3 + &(316.1s^2 + K_d G_{ocf} H_F(s)) s^2 + (1.016e0\,4 + K_p G_{ocf} H_F(s)) s + (K_i G_{ocf} H_F(s)) = 0 \end{aligned}\right\} \quad (17)$$

Therefore, (18) will be used as the baseline for system stability.

$$\Rightarrow (s+1)^3 = s^3 + 3s^2 + 3s + 1 \quad (18)$$

Equating and corresponding coefficients of the root characteristics in (17) and the assuming system stability baseline equation in 18 gives (19):

$$\left.\begin{aligned} (316.1 + K_d G_{ocf} H_F(s)) s^2 &= 3s^2 \\ (1.016e0\,4 + K_p G_{ocf} H_F(s)) s &= 3s \\ K_i G_{ocf} H_F(s) &= 1 \end{aligned}\right\} \quad (19)$$

[2] Feed forward Gain of open Loop Capacitive Accelerometer $(G_{AOL}(s))$with electronic readout circuit.

The solution for (19) (PID parameters) is given in (20).

$$\left.\begin{aligned} K_d &= \frac{(3-316.1)}{G_{ocf}H_F(s)} \\ K_p &= \frac{(3-1.016e0\,4)}{G_{ocf}H_F(s)} \\ K_i &= \frac{1}{G_{ocf}H_F(s)} \end{aligned}\right\} \quad (20)$$

Solution for $H_F(s)$ can be obtained from (11) and (12) (the feedback gain is a sensor chosen with its model proportional to the output model of the accelerometer system model, which is an electrostatic force):

$$\left.\begin{aligned} &F_{el_F} = \frac{2\varepsilon_0\varepsilon_r A V_b V_F}{{d_0}^2}; \\ &\text{obtained assuming the initial displacement is zero} \\ &a(s) = \frac{2\varepsilon_0\varepsilon_r A V_b}{m{d_0}^2} V_F(s); \\ &\text{feedback voltage } (V_b) \cong \text{system output voltage } (V_F(s)) \\ &a = \frac{2\varepsilon_0\varepsilon_r A {V_b}^2}{m{d_0}^2} \equiv V_b = \sqrt{\frac{m{d_0}^2}{2\varepsilon_0\varepsilon_r A}} \equiv H_F(s) = 1 \end{aligned}\right\} \quad (21)$$

ii. PID Auto tuning in Simulink

In the building of the accelerometer, this paper implements Simulink PID controller tuner SISO design tool. This PID Controller block output is a weighted sum of the input signal, the integral of the input signal, and the derivative of the input signal. The weights are the proportional, integral, and derivative gain parameters. A first-order pole filters the derivative action. The input of the block is typically an error signal, which is the difference between a reference signal and the system output. Parallel two-degree-of-freedom PID controller in continuous-time (time domain) with derivative filter used in tuning has a transfer function in (22):

$$\left.\begin{aligned} G_c(s) &= K_p + \frac{K_i}{s} + K_d * \frac{N3}{1+\frac{N}{s}} \\ G_c(s) &= \frac{(K_p + NK_d)s^2 + (NK_p + K_i) + K_i N}{s(s+N)} \end{aligned}\right\} \quad (22)$$

K_p =2.25E-03 , $K_i = 0.122$, K_d =4.60E-06 and N =7180.056 were the values obtained for tuning the controller.

The use of (22) in place of the analytical parallel PID structure (15) would provide a better theoretical means of tuning. The advantage of the controller model in Simulink helps in tuning by manual or automatic means to a designers choice. However, it should be noted that, the implementation of this depends on how well the plant model (capacitive accelerometer) is designed and linearized. For a non-linearized transfer function will produce no tuning option. This shows that a plant model was poorly designed.

In this paper, two forms analysis are used: comparing the time domain and frequency domain with or without the electronic readout. The next section present the various stages simulation and test of acceleration input to position (displacement) output for system validation.

[3] N: parameter that determines the amount of filtering on the derivative term on the PID structure

IV. Closed Loop Accelerometer Simulation and Results

A. Accelerometer open loop ouput

The open loop response of (6) gives the response $V_{F(s)}$ in figure 5 after an input of a step functiona(s). This shows a clear assertion of high overshoot response. Therefore, in order to solve the problem of overshoot, a PID is implored.

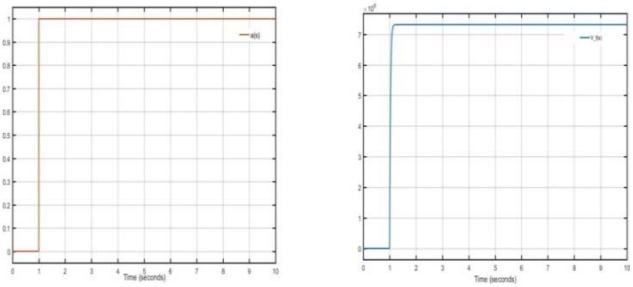

Figure 5: the open loop response of the accelerometer.

B. Simulation of entire closed loop accelerometer system in time domain

The Simulink based model in figure 6 is the accelerometer model in continuous time-function with input acceleration and all the acting forces on the accelerometer. The output of the system gives a displacement (distance/position(x)). In Figure 7, it shows the entire closed loop model with the PID controller correct the overshot of output signal in Figure 4

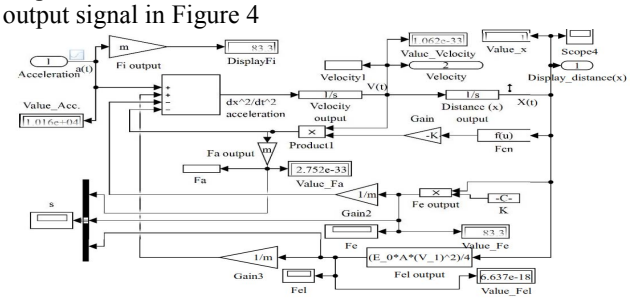

Figure 6: Simulink model of the accelerometer in continuous time-domain

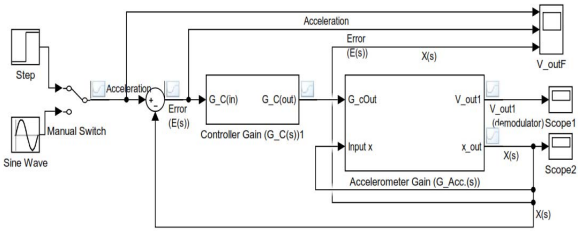

Figure 7: Entire closed loop time varying function of capacitive accelerometer

In order to simulate Figure 7, a step function signal is applied as reference i.e. acceleration($a = 1\,g$). The

simulation results show a system response (position; X(s)) and error (E(s)) in figure 8. The system produces no steady state error at 1.1 secs after using the PID controller. This shows that the acceleration of the capacitive accelerometer produces a linear dependence the system's position.

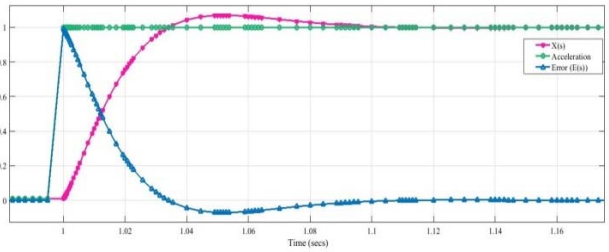

Figure 8: Acceleration (a=1 g) produces position (x=1m) and system error (e=0) at 1.1secs

In Figure 9, it shows how an increase in acceleration from 1 g to 10 g can accurately predict the measurement distance.

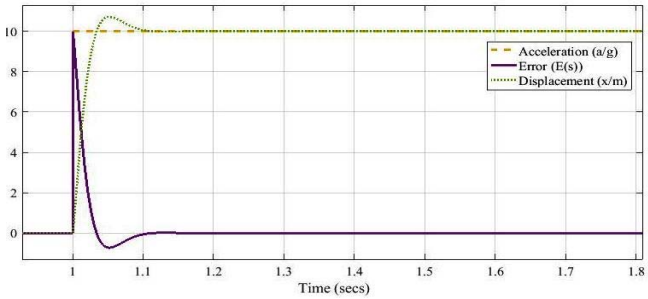

Figure 9: Acceleration (a=10 g) produces position (x=10m) and system error (e=0) at 1.1secs

C. *Final Simulation of closed loop accelerometer system in frequency domain*

The final model of the entire capacitive accelerometer is shown in figure 10. It consist of the transfer function of the PID (parallel structure with derivative filter), the mechanical part, signal detection, and the phase sensitive in one model, and the transfer function of the Low Pass Filter (LPF) having a unity feedback.

The working values for the PID controller model in equation 22 after tuning are as follows: $K_p = 2.25E-03$; $K_i = 1.23E-01s^{-1}$; $K_d = 4.60E-06s^{-1}$ and $N = 7180.056$

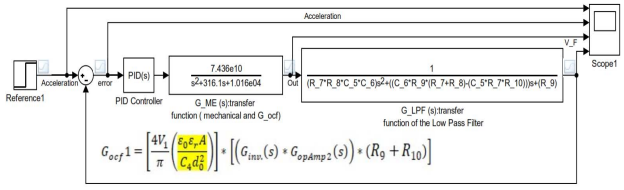

Figure 10: Entire closed loop accelerometer system with PID controller in frequency domain

The frequency domain design in figure 10 produce an observation in figure 11 after an input acceleration signal ($a = 1$ g) gives a displacement $V_F = 1$ m after an overshot lasting for less than 0.1 secs which similar to the time domain design characteristics in figure 8.

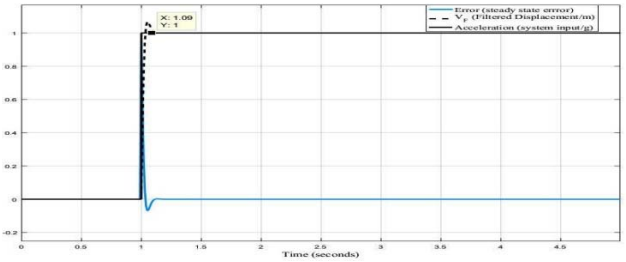

Figure 11: closed loop frequency domain capacitive accelerometer characteristics.

For a similar acceleration signal input of 10 g also produces a displacement of 10 m observation to the time domain characteristics in Figure 9. These observations show that the accelerometer design is linearly able to predict a proportional dependence of displacement of a vehicle from any varying sets of acceleration. The section would test and validate the continuous variations of acceleration input to consider in the model will be able to predict its linear dependence.

V. NUMERICAL TEST AND RESULTS VALIDATION

This section presents results on the numerical and continuous behavior of vehicle movement using sinewave signal source block in Simulink to predict the output validity of the accelerometer model. Also statistical linear dependent characteristics test is provided from the model between the acceleration and the displacement (position). A simple regression model is developed with p-value to establish the significance of whether the distance obtained from the model in linearly dependent the input.

The observation in Figure 12 and 13 represents varying acceleration (a(s)), error (e), and displacement (V_F(S)) in a continuous time function of a moving vehicle accelerometer recordings using PVA model in both time domain and frequency domain.

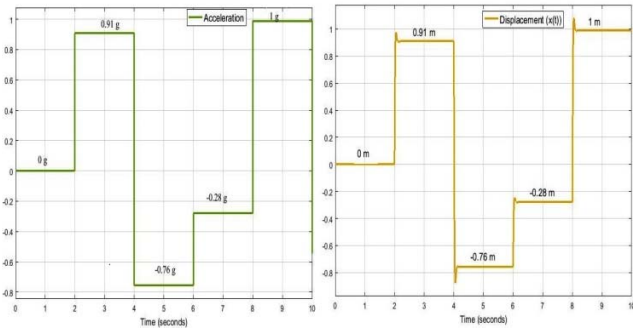

Figure 12: closed loop accelerometer test response in time domain

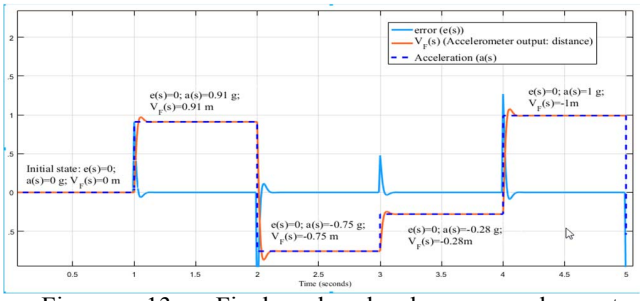

Figure 13: Final closed loop accelerometer characteristics test in frequency domain

In the test validation observation in Figure 13, the model uses acceleration function depending on time based in (23).

$$a(t) = \text{Amplitude} * \sin(\text{frequency} * \text{time} + \text{phase}) + \text{Bias} \quad (23)$$

Where $\text{Amplitude} = 1;\ \text{frequency} = 2\ H_z;\ \text{time} = 0s \leq t \leq 5s;\ \text{phase} = 0\ \text{rad}$ with sampling time of 1 s.

The accelerometer model prediction of linear dependence of displacement on acceleration for accurate response is also validated in Figure 14.

VI. Discussion

In this article, a closed loop accelerometer is designed in both frequency and time domain functions in order to aid vehicle tracking. The model uses PVA principle to convert acceleration of vehicle into distance. The model obtained a better observation using PID parallel controller with derivative filter in Simulink. The test validation of the model shows that, for any continuous time variation in accelerometer, a displacement can be predicted wit initial transient steady state error lasting less than 0.1 secs during periods of vehicles' acceleration of deceleration. However, findings obtained from the work of [26] similar linear prediction of displacement on acceleration signal input but the margin of error in much wider. For an acceleration of 4 g, produces a displacement of about 8 m. Also his model three tuning methods used was Ziegler-Nichols criteria with time domain function for the mechanical component of the accelerometer. Also, a similar finding is provided by [21] in a closed loop capacitive micro-accelerometer designed based on PSice. Reference [21] design, the relation between the feedback signal and acceleration was linearly dependent. This design showed a stability of external acceleration less than or equal to 6 g. therefore, for values above 6 g, means the system would not be stable.

The model presented in this paper is able to predict the exact acceleration signal input during the continuous time varying test at run time, $0s \leq t \leq 5s$ for $a = \pm 1\ g$ to obtain a displacement, $V_F = \pm 1\ m$ with initial transient time less than 0.1 secs.

VII. Conclusion

A closed loop capacitive accelerometer analysis and simulation with feedback based on PID controller with derivative filter is developed. The theoretical consideration underpinning the analysis is based on Position-Velocity-Acceleration (PVA) model. The closed loop accelerometer is able to produce a linear response (distance) which is dependent on any input acceleration time varying function. This model mimics how to obtain the distance of a time traveling vehicle. However, for better optimization, the accelerometer has to be modelled in a state space domain using Gaussian stochastic model where noise is factored as independent of system memory. This would also provide a better technique for sensor fusion.

Reference

[1] N. Yazdi, F. Ayazi, and K. Najafi, "Micromachined inertial sensors" Proceedings of the IEEE. 1998 Aug;86(8):1640-59.

[2] T. Mineta, S. Kobayashi, Y. Watanabe, S. Kanauchi, I. Nakagawa, E. Suganurna, and M. Esashi, "Three-axis capacitive accelerometer with uniform axial sensitivities." In *Proceedings of the International Solid-State Sensors and Actuators Conference-TRANSDUCERS'95*, vol. 2, pp. 554-557. IEEE, 1995.

[3] T. Lehtonen, and J. Thurau, "Monolithic accelerometer for 3D measurements." In *Advanced Microsystems for Automotive Applications 2004*, pp. 11-22. Springer, Berlin, Heidelberg, 2004.

[4] A. M. Dinarvand, N. Dinarvand, and M. K. Q. Joogh, "Behavioral Modeling and Simulation of an Open-loop MEMS Capacitive Accelerometer with the MATLAB/SIMULINK." *parameters* 7 (2014): 2

[5] B. Guldimann, P. Dubois, P. A. Clere, and D. Rooji, "Fiber Optic—MEMS Accelerometer with high mass displacement resolution." In *Transducers' 01 Eurosensors XV*, pp. 438-441. Springer, Berlin, Heidelberg, 2001.

[6] M. Paavola, M. Kamarainen, J. A. Jarvinen, M. Saukoski, M. Laiho, and K. A. Halonen, "A micropower interface ASIC for a capacitive 3-axis micro-accelerometer." *IEEE Journal of Solid-State Circuits* 42, no. 12 (2007): 2651-2665.

[7] R. C. Dorf, and R. H. Bishop, *Modern control systems*. Pearson, 2011.

[8] Matsumoto, Y., & Esashi, M. (1993). Integrated silicon capacitive accelerometer with PLL servo technique. Sensors and Actuators A: Physical, 39(3), 209-217.

[9] W. Kuehnel, and S. Sherman, "A surface micromachined silicon accelerometer with on-chip detection circuitry." *Sensors and Actuators A: Physical* 45, no. 1 (1994): 7-16.

[10] B. E. Boser, and R. T. Howe, "Surface micromachined accelerometers." *IEEE Journal of solid-state circuits* 31, no. 3 (1996): 366-375.

[11] C. Hierold, A. Hildebrandt, U. Na, T. Scheiter, B. Mensching, M. Steger, and R. Tielert, "A pure CMOS surface-micromachined integrated accelerometer." *Sensors and Actuators A: Physical* 57, no. 2 (1996): 111-116.

[12] N. Yazdi, & K. Najafi, "An all-silicon single-wafer micro-g accelerometer with a combined surface and bulk micromachining process." *Journal of Microelectromechanical systems* 9, no. 4 (2000): 544-550.

[13] H. Luo, G. Zhang, L. R. Carley, and G. K. Fedder, "A post-CMOS micromachined lateral accelerometer." *Journal of Microelectromechanical systems* 11, no. 3 (2002): 188-195.

[14] B. V. Amini, and F. Ayazi, "A 2.5-V 14-bit/spl Sigma//spl Delta/CMOS SOI capacitive accelerometer." *IEEE Journal of Solid-State Circuits* 39, no. 12 (2004): 2467-2476.

[15] L. M. Roylance, and J. B. Angell, "A batch-fabricated silicon accelerometer." *IEEE Transactions on Electron Devices* 26, no. 12 (1979): 1911-1917.

[16] Allen, H. V., Terry, S. C., & De Bruin, D. W. (1989). Accelerometer systems with self-testable features. Sensors and Actuators, 20(1-2), 153-161.

[17] K. Yamada, K. Higuchi, and H. Tanigawa, "A novel silicon accelerometer with a surrounding mass structure." *Sensors and Actuators A: Physical* 21, no. 1-3 (1990): 308-311.

[18] R. Hiratsuka, D. C. Van Duyn, T. Otaredian, P. De Vries, and P. M. Sarro, "Design considerations for the thermal accelerometer." *Sensors and Actuators A: Physical* 32, no. 1-3 (1992): 380-385.

[19] A. M. Leung, J. Jones, E. Czyzewska, J. Chen, and B. Woods, "Micromachined accelerometer based on convection heat transfer." In *Proceedings MEMS 98. IEEE. Eleventh Annual International Workshop on Micro Electro Mechanical Systems. An Investigation of Micro Structures, Sensors, Actuators, Machines and Systems (Cat. No. 98CH36176*, pp. 627-630. IEEE, 1998.

[20] A. Kazama, T. Aono, and R. Okada, "Stress relaxation mechanism with a ring-shaped beam for a piezoresistive three-axis accelerometer." *Journal of Microelectromechanical Systems* 22, no. 2 (2012): 386-394.

[21] P. Chen, J. Bai, S. Lou, Q. Lu, D. Han, and X. Jiao, (2017, June). "Design of the closed-loop capacitive microaccelerometer based on PSpice." In *2017 First International Conference on Electronics Instrumentation & Information Systems (EIIS)*, pp. 1-4. IEEE, 2017.

[22] K. N. Khamil, K. S. Leong, N. B. Mohamad, N. Soin, and N. Saba, "Analysis of mems accelerometer for optimized sensitivity." *International Journal of Engineering&Technology* 6, no. 6 (2014): 2705-2711.

[23] M. Kraft, C. P. Lewis, and T. G. Hesketh "Control system design study for a micromachined accelerometer." *IFAC Proceedings Volumes* 30, no. 21 (1997): 139-143.

[24] M. Liu, G. Zhang, J. Dong, and C. Zhao, "A novel digital closed loop MEMS accelerometer utilizing a charge pump." *Sensors*16, no. 3 (2016): 389.

[25] Y. Terzioglu, S. E. Alper, K. Azgin, & T. Akin, "A capacitive MEMS accelerometer readout with concurrent detection and feedback using discrete components." In *2014 IEEE/ION Position, Location and Navigation Symposium-PLANS 2014*, pp. 12-15. IEEE, 2014.

[26] G. L. Teodor, "The Matlab/Simulink modeling and numerical simulation of an analogue capacitive micro-accelerometer. Part 2: Closed loop." In 2008 International Conference on Perspective Technologies and Methods in MEMS Design, pp. 115-121. IEEE, 2008.